

Re-examining the Too-Big-To-Fail Problem for Dark Matter Haloes with Central Density Cores

Go Ogiya^{1,2,3*} and Andreas Burkert^{1,2†}

¹*Universitäts-Sternwarte München, Scheinerstraße 1, D-81679 München, Germany*

²*Max-Planck-Institut für extraterrestrische Physik, Postfach 1312, Giessenbachstraße, D-85741 Garching, Germany*

³*Graduate School of Pure and Applied Science, University of Tsukuba, 1-1-1, Tennodai, Tsukuba, Ibaraki, 305-8577, Japan*

Accepted ***. Received ***, in original form 2014 ***

ABSTRACT

Recent studies found the masses of dark matter (DM) subhaloes which surround nearby dwarf spheroidal galaxies (dSphs) to be significantly lower than those of the most massive subhaloes expected around Milky Way sized galaxies in cosmological simulations, the so called “too-big-to-fail” (TBTf) problem. A caveat of previous work has been that dark substructures were assumed to contain steep density cusps in the center of DM haloes even though the central density structure of DM haloes is still under debate. In this study, we re-examine the TBTf problem for models of DM density structure with cores or shallowed cusps. Our analysis demonstrates that the TBTf problem is alleviated as the logarithmic slope of the central cusp becomes shallower. We also derive the critical logarithmic slope of the central density required in order to solve the TBTf problem.

Key words: cosmology: dark matter – galaxies: evolution – galaxies: formation – galaxies: dwarf – galaxies: Local Group

1 INTRODUCTION

The local universe is a good site to test cosmological models. The current standard paradigm, the Λ cold dark matter (Λ CDM) model, reproduces the large-scale properties of the universe successfully (e.g., Tegmark et al. 2004; Eisenstein et al. 2005; Hinshaw et al. 2007). However, some serious discrepancies between the Λ CDM prediction and observations have been identified in the local universe and are known as still remaining small-scale problems of Λ CDM cosmology.

For example, recent studies revealed that the masses of the most massive dark matter (DM) subhaloes expected around Milky Way (MW) sized haloes in cosmological dissipationless simulations are much larger than those of subhaloes which surround nearby classical dwarf spheroidal galaxies (dSphs), the so called too-big-to-fail (TBTf) problem (Boylan-Kolchin, Bullock & Kaplinghat 2011, 2012; Garrison-Kimmel et al. 2014). Massive satellite haloes are more likely to host galaxies than less-massive haloes because of their deeper potential well. These theoretically expected massive satellites that are however not observed are called “massive failures”. This problem also means a crisis for the abundance matching technique which

assumes that the stellar mass of galaxies is a monotonic function of halo mass.

Independent of the TBTf problem, the discrepancy about the inner mass-density structure of DM haloes, the core-cusp problem, has been under debate for two decades. Cosmological N -body simulations, based on the CDM model, predict the existence of a divergent density distribution, a cusp, in the centre of haloes (Navarro, Frenk & White 1997; Fukushige & Makino 1997; Moore et al. 1999; Jing & Suto 2000; Navarro et al. 2010; Ishiyama et al. 2013, and references therein). On the other hand, galaxies dynamically dominated by DM such as dwarf and low-surface-brightness galaxies disagree with such a cuspy mass-density structure and have a constant density core (e.g., Moore 1994; de Blok et al. 2001; Swaters et al. 2003; Spekkens, Giovanelli & Haynes 2005; van Eymeren et al. 2009; Oh et al. 2011). The cuspy profiles are derived from DM only simulations and the fluctuations in the gravitational potential due to baryonic dynamical processes are supposed to alter the inner structure of DM haloes. Such fluctuations could be induced by violent gas outflows, driven by supernova- and/or AGN feedback (Navarro, Eke & Frenk 1996; Ogiya & Mori 2011, 2012; Pontzen & Governato 2012; Teyssier et al. 2013, and references therein) or by dynamical friction of gas or stellar clumps, spiraling into the center (e.g., El-Zant, Shlosman & Hoffman 2001; Ma & Boylan-Kolchin

* E-mail: ogiya@mpe.mpg.de

† Max-Planck Fellow

2004; Tonini, Lapi & Salucci 2006; Goerdt et al. 2010; Inoue & Saitoh 2011). Ogiya et al. (2014) showed that the cusp-to-core transformation reproduces observed scaling relations of DM cores well.

The inner density structure of the TBTF haloes is still a matter to debate. Some studies advocate the existence of a density core in the center of some dSphs (e.g., Walker & Peñarrubia 2011; Agnello & Evans 2012; Jardel & Gebhardt 2012; Hayashi & Chiba 2012; Amorisco, Agnello & Evans 2013). On the other hand, it is still difficult to distinguish cored profiles from cuspy ones (e.g., Koch et al. 2007; Walker et al. 2009; Breddels & Helmi 2013; Richardson & Fairbairn 2013; Strigari, Frenk & White 2014). These difficulties are expected to be solved by ongoing and forthcoming observations such as GAIA (de Bruijne 2012) and the Subaru Hyper-Suprime-Camera (Takada 2010).

Even though the inner density profile of dSphs is uncertain, previous work has assumed cuspy models for DM haloes. The question then arises how a more cored profile would affect the TBTF puzzle. The TBTF problem is defined in the $V_{\max} - R_{\max}$ plane, where V_{\max} is the maximum circular velocity defined as

$$V_{\max} = \max [V_c(r)] = \max \left[\sqrt{\frac{GM(r)}{r}} \right], \quad (1)$$

with R_{\max} the radius at which V_{\max} is attained, G is the gravitational constant and $M(r)$ is the mass within radius r , respectively. The assumption of a core should strongly affect the conclusion because V_{\max} and R_{\max} depend on the mass profile of DM halo models (Garrison-Kimmel et al. 2013; Madau, Shen & Governato 2014).

The motivation of this study is to re-examine the TBTF problem for models of DM density profiles with cores or shallowed cusps. We find that the TBTF problem is alleviated as the logarithmic slope of the central cusp becomes shallower. Our analysis demonstrates that for cored dark haloes the TBTF problem can be solved and it provides the steepest, allowed logarithmic slope in order to avoid a TBTF problem. This paper is organized as follows. The procedures and assumptions of the analysis are described in Section 2. In Section 3, we present results of the analysis. We discuss and summarize the results in Section 4 and 5, respectively.

2 ANALYSIS

Following Boylan-Kolchin, Bullock & Kaplinghat (2011, hereafter B11), we compare $V_{\max} - R_{\max}$ values constrained by observations with theoretical predictions.

2.1 Constraint by observations

Along the line of B11, we constrain V_{\max} and R_{\max} by the kinetic data derived by Wolf et al. (2010), the deprojected half-light radii, $R_{1/2}$, and the dynamical masses within $R_{1/2}$ of dSphs, $M_{1/2}$. DSphs are dynamically dominated by DM even within $R_{1/2}$ (e.g., Mateo 1998) and this property allows us to regard $M_{1/2}$ as DM mass. General models of DM mass-density profile are characterized by two parameters. For the Navarro-Frenk-White (NFW) model (Navarro, Frenk & White 1997),

$$\rho(r) = \frac{\rho_s r_s^3}{r(r+r_s)^2}, \quad (2)$$

these parameters are ρ_s and r_s , the scale density and length, respectively. The mass profile is given by

$$M(r) = 4\pi\rho_s r_s^3 \left[\ln \left(1 + \frac{r}{r_s} \right) - \frac{(r/r_s)}{1 + (r/r_s)} \right], \quad (3)$$

for NFW haloes. Since only the enclosed mass within $R_{1/2}$ is obtained by observations, it is impossible to uniquely determine the characteristics for each DM halo. In the wake of B11, we take account of the 1σ confidence range for the observational data, $M_{1/2}$ and $R_{1/2}$.

We assume not only NFW-type models but also more generalised DM density profiles to re-examine the TBTF problem. As described in Section 1, the inner density structure of dSphs is an open question. One of the models which we apply to the analysis is the so called α -model,

$$\rho(r) = \frac{\rho_0 r_0^3}{r^\alpha (r + r_0)^{3-\alpha}}, \quad (4)$$

where α , ρ_0 and r_0 mean the logarithmic slope of the central cusp and the scale density and length, respectively. Here, $\alpha = 1$ corresponds to the NFW model and the model of $\alpha = 0$ has a central core. In this study, we consider models which satisfy $0 \leq \alpha \leq 1$. The mass profile for the α -model is

$$M(\alpha; r) = \frac{4\pi\rho_0 r_0^3}{3-\alpha} \left(\frac{r}{r_0} \right)^{3-\alpha} \times {}_2F_1 \left[3-\alpha, 3-\alpha, 4-\alpha; -\left(\frac{r}{r_0} \right) \right], \quad (5)$$

(Tsuchiya, Mori & Nitta 2013). Here, ${}_2F_1[3-\alpha, 3-\alpha, 4-\alpha; -(r/r_0)]$ is Gauss's hypergeometric function.

We also check for the Burkert model

$$\rho(r) = \frac{\rho_0 r_0^3}{(r + r_0)(r^2 + r_0^2)}, \quad (6)$$

which is a cored model and well reproduces the mass-density structure of dwarf and spiral galaxies (Burkert 1995; Salucci & Burkert 2000). The mass profile is given by

$$M(r) = \pi\rho_0 r_0^3 \left[-2 \arctan \left(\frac{r}{r_0} \right) + 2 \ln \left\{ 1 + \left(\frac{r}{r_0} \right) \right\} + \ln \left\{ 1 + \left(\frac{r}{r_0} \right)^2 \right\} \right], \quad (7)$$

for Burkert haloes (Mori & Burkert 2000).

2.2 Prediction for properties of dark haloes

In order to compare the observational constraints with theoretical predictions we assume that DM haloes form following an NFW profile initially. The structure of an NFW halo depends on the concentration parameter $c \equiv r_{200}/r_s$, where r_{200} is the virial radius. Inside of r_{200} , the mean density of the DM halo is 200 times the critical density of the universe. The virial mass, M_{200} is related to r_{200} by $M_{200} \equiv (4\pi/3)200\rho_{\text{crit}}(1+z)^3 r_{200}^3$ where ρ_{crit} and z are the critical density of the universe and redshift, respectively. The concentration parameter, c is a function of M_{200} and z . We adopt $c(M_{200}, z)$ as proposed by Prada et al. (2012) which

is appropriate down to $M_{200} \sim 10^8 M_\odot$ which is the mass scale of dwarf galaxies (Ogiya et al. 2014).

We then assume that the central cusp of the NFW halo is shallowed by some dynamical process and the density profile transforms into Eq. (4) or (6). We impose two physical conditions in order to determine the two free parameters ρ_0 and r_0 . The first one is the conservation of the virial mass, $M_{200} = M(r_{200})$. The second condition is the conservation of the mass-density in the outskirts. This is reasonable if the cusp shallowing is caused by fluctuations in the gravitational potential driven by baryonic flows in the inner dark halo regions. From equations (2), (4) and (6), the following should then be satisfied,

$$\rho_s r_s^3 = \rho_0 r_0^3. \quad (8)$$

We also have to define a redshift at which the central cusp has been shallowed, z_s , and assume that the parameters of DM haloes, ρ_0 and r_0 , are conserved until a redshift, z' . Fig. 1 shows the resultant density profiles of DM haloes after the process of the cusp shallowing. The dark haloes have the identical initial NFW configuration. For the α -model, the central cusp is shallower and the central density of DM haloes decreases the smaller α . The core is even larger and the central density becomes even smaller in Burkert haloes, compared to the $\alpha = 0$ model.

We now test the TBTF problem and its dependence on the DM halo profile by focussing on the satellite system of the MW. Press & Schechter (1974) have established a formalism to derive the number density of DM haloes for given halo mass and redshift. The predicted number densities well match the results of cosmological N -body simulations (e.g., Sheth & Tormen 1999). Subsequent studies extended the formalism and obtained useful expressions. Bower (1991) obtained a formula to compute the mass fraction of elements which were dark haloes of mass M_1 at z_1 and have merged to form a larger dark halo of mass $M_0 > M_1$ by $z_0 < z_1$. The average number of progenitors, N_{prg} is given by

$$N_{\text{prg}}(M_0, z_0 | M_1, z_1) = \sqrt{\frac{2}{\pi}} \frac{M_0}{M_1} \frac{\sigma_1(\delta_1 - \delta_0)}{(\sigma_1^2 - \sigma_0^2)^{3/2}} \times \exp \left[-\frac{(\delta_1 - \delta_0)^2}{2(\sigma_1^2 - \sigma_0^2)} \right] \left| \frac{d\sigma_1}{dM_1} \right|, \quad (9)$$

where δ_n and σ_n ($n = 0, 1$) are the linear overdensity and the linear rms fluctuation of the density field, respectively. The linear overdensity, δ_n is defined by $\delta_n = \delta_c / D(z_n)$ where $\delta_c = 1.69$ is the critical overdensity to collapse and $D(z_n)$ is the linear growth factor measured at z_n . The linear rms fluctuation of the density field, σ_n is a monotonically decreasing function of halo mass. Lacey & Cole (1993) derived a conditional probability, $P'(M', z' | M_{200}, z_s)$, that a dark halo makes a transition from $M = M_{200} < M'$ to $M > M'$ within a time frame from z_s to $z' < z_s$. The inverse probability which corresponds to the probability that a dark halo does not make the transition is given by $P(M', z' | M_{200}, z_s) = 1 - P'(M', z' | M_{200}, z_s)$. P can be regarded as the fraction of DM haloes with masses M_{200} at z_s that survive until z' without substantial growth of their mass. Combining N_{prg} and P , we derive the expected number of surviving DM haloes for given time and environment.

In order to compute N_{prg} and P , some cosmological parameters and the dynamical mass of the MW, M_{MW}

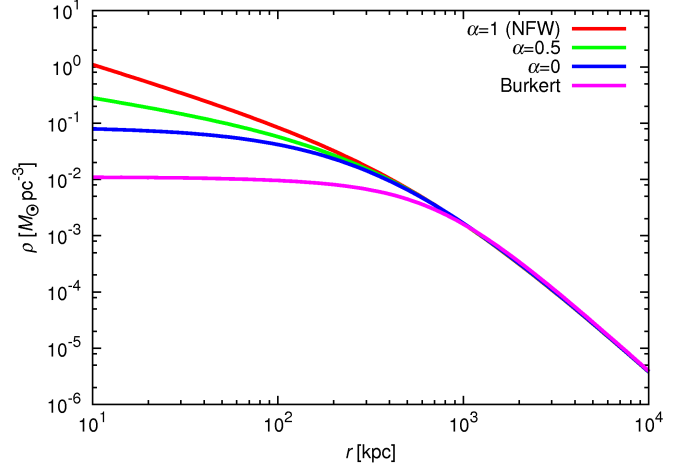


Figure 1. Density profile of DM haloes with $M_{200} = 10^8 M_\odot$ and $z_s = 0$ after the process of the cusp shallowing.

are required. The cosmological parameters in the following analysis are determined by Komatsu et al. (2011). For the MW, we adopt the dynamical mass $M_{\text{MW}} = 2.43 \times 10^{12} M_\odot$ (Li & White 2008). We compute the number of mass elements contained in the MW halo which were DM haloes with M_{200} at z_s by using Eq. (9), i.e. $N_{\text{prg}}(M_{\text{MW}}, 0 | M_{200}, z_s)$. The surviving satellite haloes in the MW halo are defined as dark haloes whose mass does not reach $M' = 2M_{200}(z_s)$ until $z' = 0$. We assume that DM haloes which satisfy this condition are surviving as independent haloes and halo properties have been conserved. The number of subhaloes of the MW with halo mass, M_{200} , and redshift for cusp shallowing, z_s , is calculated by

$$N_0(M_{200}, z_s) = N_{\text{prg}}(M_{\text{MW}}, 0 | M_{200}, z_s) \times P(2M_{200}, 0 | M_{200}, z_s). \quad (10)$$

3 RESULTS

In order to re-examine the TBTF problem for DM density models with central cores or shallowed cusps, we parametrise the inner density structure of DM haloes in the analysis. In Fig. 2, we compare the constraints on DM subhaloes obtained from kinematic data of nearby dSphs with the predicted properties of DM haloes for various models of DM density profiles. Each panel shows the results for an NFW model with $\alpha = 1$, $\alpha = 0.5, 0$ and a Burkert profile. The observed dSphs of the MW lie within the shaded regions. Red lines show the contour where of expected number of satellites around the MW at the present time is unity, i.e. $N_0 = 1$ (see equation 10). Satellites should be detected at least all the way down to this region. Black lines show the theoretically predicted properties of dark haloes with inner profiles as introduced in Section 2. The size of the unshaded area between the red line and shaded region correlates with the number of massive failures.

Panel (a) corresponds to NFW profiles and confirms the results of previous studies (cf. Fig. 2 of B11). We find a large likelihood for massive failures for models with a steep central cusp. The observed dSphs are distributed along by the bottom part of the shaded region. They however do not

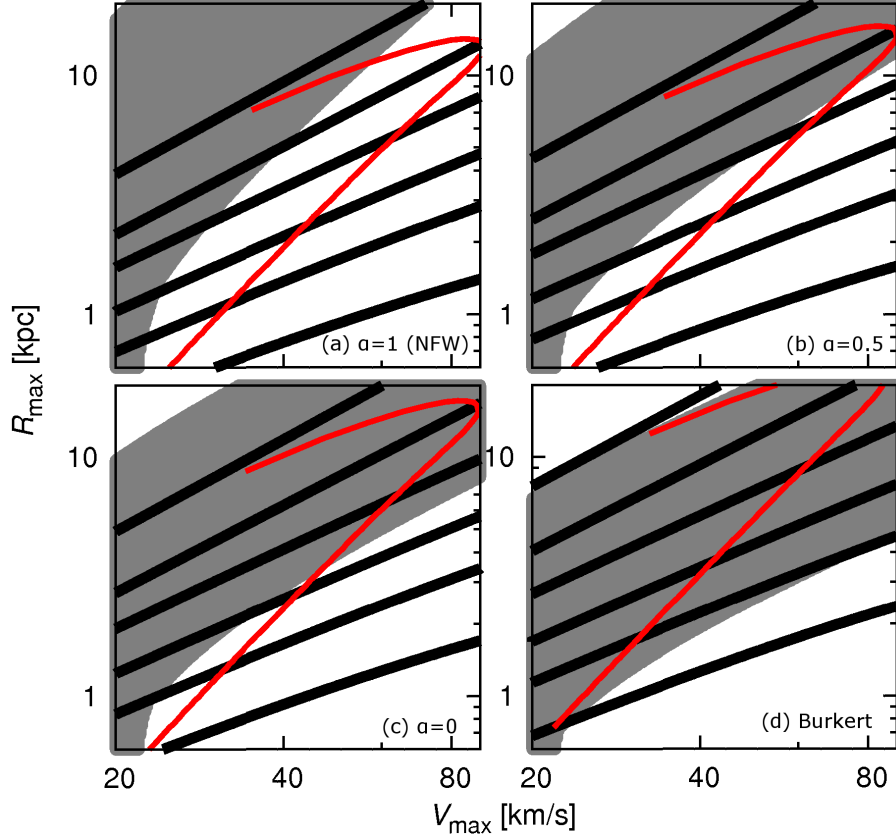


Figure 2. Comparison between observationally constrained and theoretically predicted properties of DM haloes in the $V_{\max} - R_{\max}$ plane. Each panel depicts the results assuming various models of DM density profiles. Shaded regions represent the locations of observed dSphs around the MW. Black lines are the predicted properties of DM haloes assuming NFW haloes transformed into mass-density models with central cores or shallowed cusps. From the top black lines to the bottom ones, they show results for redshifts $z_s = 0, 1, 3, 5, 7$ and 10, respectively. For given V_{\max} , R_{\max} increases with decreasing z_s . Red lines represent the contours where the expected number of dSphs around the MW approaches unity: $N_0 = 1$.

extend into the unshaded region above the red line. Fig. 2 also demonstrates that the size of the area between the red line and shaded region decreases, i.e., the TBTF problem is alleviated, as the central cusp is shallowed and the central density of DM haloes decreases.

To understand the results of the analysis, we need to consider the meaning of the maximum circular velocity, V_{\max} which can be rewritten as

$$\frac{V_c(r)^2}{G} = \frac{M(r)}{r} \sim \frac{dM(r)}{dr} = 4\pi r^2 \rho(r), \quad (11)$$

for spherical systems. For profiles with $\alpha > 0$, it increases around the center, reaches a peak at R_{\max} where the density distribution is quasi-isothermal with a logarithmic slope of -2 and then declines in the outskirts where $\rho \propto r^{-3}$. R_{\max} therefore is proportional to the scale length, r_0 and V_{\max} is a function of the product, $\rho_0 r_0^3$.

The black lines in Fig. 2 show the expected correlation of R_{\max} versus V_{\max} for satellites with various redshifts at which the central cusp has been shallowed, z_s . As discussed above, the maximum circular velocity, V_{\max} depends on the product, $\rho_0 r_0^3$. This is one of the conditions imposed on the core formation process: the conservation of the mass-density in the outskirts of DM haloes, Eq. (8). Therefore, V_{\max} is almost conserved during the shallowing process. Shallowing

the central cusps leads to an expansion of the central region of DM haloes. As a consequence, the radius R_{\max} where the logarithmic slope of the density profile equals the isothermal value of -2 moves outward. The amount of change in R_{\max} increases with increasing difference between the initial cuspy profile and the resultant core or shallowed cusp profile.

The shaded regions show the location of observed dSphs. They move to smaller R_{\max} as the logarithmic slope of the central cusp becomes shallower. The DM haloes have the same V_{\max} , i.e., approximately the same $\rho_0 r_0^3$ values for different density profiles. In order to satisfy the condition that the mass, enclosed within the half-light-radii $M_{1/2}$, is as observed, models with central cores or shallow cusps need higher central densities than those with steep cusps. This leads the scale length of DM haloes, r_0 , to decrease. Since R_{\max} is proportional to r_0 , the range of R_{\max} occupied by observed dSphs decreases as the logarithmic slope of the central cusp becomes shallower.

Next, we estimate the number of massive failures around the MW at the present time, N_{mf} , and derive the critical logarithmic slope to solve the TBTF problem, α_{crit} . By integrating $N_0(M_{200}, z_s)$ in the unshaded region below the shaded ones, the number of massive failures can be cal-

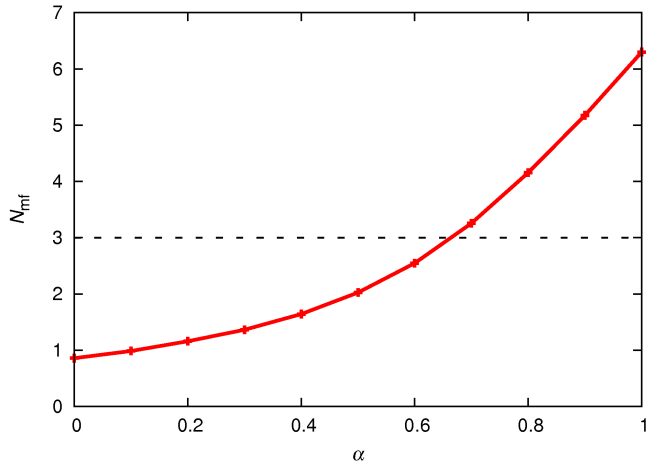


Figure 3. Number of massive failures, N_{mf} as a function of the logarithmic slope of the central cusp, α . The black line corresponds to $N_{\text{mf}} = 3$.

culated,

$$N_{\text{mf}} = \int N_0(M_{200}, z_s) d \ln S, \quad (12)$$

where $d \ln S$ is an element area in the logarithmic $V_{\text{max}} - R_{\text{max}}$ plane. This definition of massive failures follows B11 and Boylan-Kolchin, Bullock & Kaplinghat (2012) and is referred to as “strong massive failures” in Garrison-Kimmel et al. (2014).

Fig. 3 demonstrates that the number of massive failures, N_{mf} decreases as the logarithmic slope of the central cusp, α becomes shallower. More than 6 massive failures exist around the MW if DM haloes follow NFW density profiles. This is consistent with the results of recent studies, based on numerical simulations (cf. Fig. 3 of Boylan-Kolchin, Bullock & Kaplinghat 2012). 3 satellite galaxies more massive than dSphs exist around the MW, i.e. the Large- and Small Magellanic Clouds (e.g. van der Marel 2006; Bekki & Stanimirović 2009) and the Sagittarius dwarf galaxy. The Sagittarius dwarf galaxy is interacting with the MW and the stripped stars are observed as the Sagittarius stellar stream (Majewski et al. 2003). Niederste-Ostholt et al. (2010) estimate that the dynamical mass of the progenitor of the Sagittarius dwarf galaxy is $\sim 10^{10} M_{\odot}$. Therefore, we define the condition to solve the TBTF problem as $N_{\text{mf}} \leq 3$. Fig. 3 shows that N_{mf} falls below 3 in $\alpha < \alpha_{\text{crit}} = 0.6$. If NFW haloes transform into Burkert haloes, N_{mf} decreases to 0.035 and the TBTF problem is completely solved.

4 DISCUSSION

4.1 Potential of stellar feedback to solve the small-scale problems

The results of the analysis indicate that the TBTF problem is closely connected to the flattening of the central cusp, i.e., solving the core-cusp problem. Baryonic physics has been suggested as a unified solution for DM small-scale problems (Del Popolo et al. 2014). A change in the galactic potential

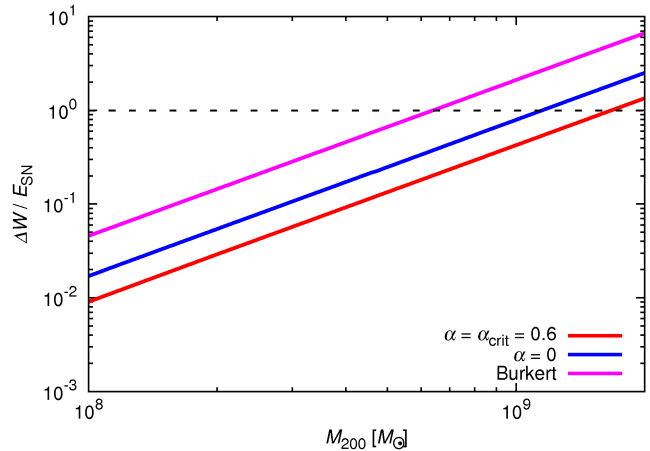


Figure 4. Ratio between the available energy of supernova feedback, E_{SN} and the required energy ΔW to transform cuspy haloes into haloes with central cores or shallowed cusps as a function of halo mass, M_{200} . Red, blue and magenta lines represent results for models of $\alpha = \alpha_{\text{crit}} = 0.6$, $\alpha = 0$ and Burkert profile, respectively. The black, dashed line corresponds to $\Delta W = E_{\text{SN}}$.

driven by stellar feedback might be a promising solution to decrease the central density of DM haloes.

Peñarrubia et al. (2012) calculated the required energy to transform cuspy haloes into cored haloes and compared it with the available energy from supernova feedback. Following this work, we define $\Delta W \equiv |W_{\text{ini}} - W_{\text{fin}}|/2$, where W_{ini} and W_{fin} is the potential energy of the initial NFW halo and corresponding halo with central core or shallowed cusp, respectively. A Salpeter initial mass function (Salpeter 1955) is adopted to estimate the energy released by Type II supernovae (SNe II), E_{SN} . The luminosity of dSphs around the MW is at least 10^5 times the solar value (Irwin & Hatzidimitriou 1995). We therefore adopt $10^5 M_{\odot}$ for the stellar mass of galaxies and assume that a SN releases 10^{51} erg of energy. The upper and lower mass limit of stars are set to $100 M_{\odot}$ and $0.1 M_{\odot}$, respectively. The lower mass limit of stars which will explode as SNe II is assumed to be $8 M_{\odot}$.

According to Salvadori, Ferrara & Schneider (2008), the virial masses of nearby dSphs are $\sim 10^8 M_{\odot}$. Here, we analyse DM haloes whose central cusps have been shallowed at $z_s = 5$. Considering higher redshift, ΔW increases because DM haloes are denser than those of lower redshifts. SN feedback provides haloes on and below the black, dashed line in Fig. 4 with sufficient energy to transform steep cusps into flat cores or shallowed cusps. This result highlights the potential of stellar feedback to solve the small-scale problems of Λ CDM cosmology. Whether this solution is reasonable depends critically on the fraction of SN energy that can be transferred to the DM haloes. Fig. 4 indicates the required fraction of energy transferred into the DM distribution for each model. Despite of a lot of efforts this efficiency is still uncertain. More studies are needed in order to better understand the formation process of cores in dwarf satellite haloes.

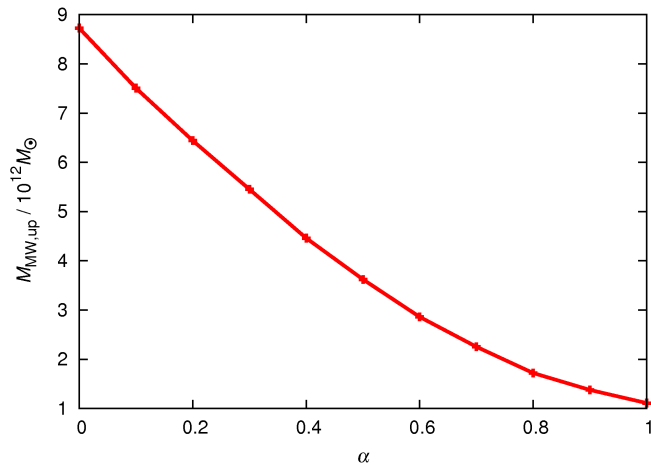


Figure 5. Upper mass limit of the MW halo derived from the condition to avoid the TBTF problem, $M_{\text{MW,up}}$ as a function of the logarithmic slope of the central cusp, α .

4.2 Dynamical mass of the Milky Way

Another important constraint for the TBTF problem is the dynamical mass of the MW. Using the results of cosmological N -body simulations, Wang et al. (2012) demonstrate that the number of subhaloes which can be regarded as massive failures increases roughly linearly with the mass of the host haloes. Eq. (9) explains the dependence. Cautun et al. (2014) constrain the dynamical mass of the MW halo by the condition to match the number of observed satellite galaxies around the MW. The upper mass limit is determined from the condition to avoid the TBTF problem, i.e. the number of subhaloes which are more massive than dSphs should be equal to or less than 3.

Following this condition, we derive the upper mass limit of the MW halo for respective density models of subhaloes. Fig. 5 shows the upper mass limit of the MW halo required in order to avoid the TBTF problem, $M_{\text{MW,up}}$ as a function of the logarithmic slope of the central cusp, α . $M_{\text{MW,up}}$ for the NFW model ($\alpha = 1$), $\approx 1.1 \times 10^{12} M_{\odot}$ is consistent with the constraint obtained by Cautun et al. (2014). The allowed ranges of the MW halo mass are extended as the logarithmic slope of the central cusp becomes shallower. Therefore, a precise determination of the inner mass-density structure of satellite galaxies could provide interesting constraints for the host halo mass.

5 SUMMARY

In this study, we re-examined one of the small-scale problems in Λ CDM cosmology, the TBTF problem. The central density structure of DM haloes is still an open question for dSphs. Previous studies have assumed models of DM density profiles with steep cusps, such as the NFW profile. This motivated us to re-examine the problem for models of DM density structure with central cores or shallowed cusps. Our analysis demonstrates that the TBTF problem is alleviated as the logarithmic slope of the central cusp becomes shallower and it reduces to less than 3 failures for slopes shallower than $\alpha_{\text{crit}} = 0.6$. Ongoing and forthcoming ob-

servational projects are expected to provide us data with sufficient quality to determine the values of α in the center of DM haloes, surrounding nearby dSphs.

ACKNOWLEDGMENTS

This work was supported in part by Grant-in-Aid for JSPS Fellows (25-1455 GO) and JSPS Grants-in-Aid for Scientific Research: (A) (21244013) and (C) (18540242). AB acknowledges support from the cluster of excellence “Origin and Structure of the Universe”.

REFERENCES

- Agnello A., Evans N. W., 2012, *ApJ*, 754, L39
- Amorisco N. C., Agnello A., Evans N. W., 2013, *MNRAS*, 429, L89
- Bekki K., Stanimirović S., 2009, *MNRAS*, 395, 342
- Bower R. G., 1991, *MNRAS*, 248, 332
- Boylan-Kolchin M., Bullock J. S., Kaplinghat M., 2011, *MNRAS*, 415, L40
- Boylan-Kolchin M., Bullock J. S., Kaplinghat M., 2012, *MNRAS*, 422, 1203
- Breddels M. A., Helmi A., 2013, *A&A*, 558, A35
- Burkert A., 1995, *ApJ*, 447, L25
- Cautun M., Frenk C. S., van de Weygaert R., Hellwing W. A., Jones B. J. T., 2014, *ArXiv e-prints*
- de Blok W. J. G., McGaugh S. S., Bosma A., Rubin V. C., 2001, *ApJ*, 552, L23
- de Bruijne J. H. J., 2012, *Ap&SS*, 341, 31
- Del Popolo A., Lima J. A. S., Fabris J. C., Rodrigues D. C., 2014, *J. Cosmology Astropart. Phys.*, 4, 21
- Eisenstein D. J. et al., 2005, *ApJ*, 633, 560
- El-Zant A., Shlosman I., Hoffman Y., 2001, *ApJ*, 560, 636
- Fukushige T., Makino J., 1997, *ApJ*, 477, L9
- Garrison-Kimmel S., Boylan-Kolchin M., Bullock J. S., Kirby E. N., 2014, *ArXiv e-prints*
- Garrison-Kimmel S., Rocha M., Boylan-Kolchin M., Bullock J. S., Lally J., 2013, *MNRAS*, 433, 3539
- Goerdt T., Moore B., Read J. I., Stadel J., 2010, *ApJ*, 725, 1707
- Hayashi K., Chiba M., 2012, *ApJ*, 755, 145
- Hinshaw G. et al., 2007, *ApJS*, 170, 288
- Inoue S., Saitoh T. R., 2011, *MNRAS*, 418, 2527
- Irwin M., Hatzidimitriou D., 1995, *MNRAS*, 277, 1354
- Ishiyama T. et al., 2013, *ApJ*, 767, 146
- Jardel J. R., Gebhardt K., 2012, *ApJ*, 746, 89
- Jing Y. P., Suto Y., 2000, *ApJ*, 529, L69
- Koch A., Kleya J. T., Wilkinson M. I., Grebel E. K., Gilmore G. F., Evans N. W., Wyse R. F. G., Harbeck D. R., 2007, *AJ*, 134, 566
- Komatsu E. et al., 2011, *ApJS*, 192, 18
- Lacey C., Cole S., 1993, *MNRAS*, 262, 627
- Li Y.-S., White S. D. M., 2008, *MNRAS*, 384, 1459
- Ma C.-P., Boylan-Kolchin M., 2004, *Physical Review Letters*, 93, 021301
- Madau P., Shen S., Governato F., 2014, *ApJ*, 789, L17
- Majewski S. R., Skrutskie M. F., Weinberg M. D., Ostriker J. C., 2003, *ApJ*, 599, 1082
- Mateo M. L., 1998, *ARA&A*, 36, 435

- Moore B., 1994, *Nature*, 370, 629
- Moore B., Quinn T., Governato F., Stadel J., Lake G., 1999, *MNRAS*, 310, 1147
- Mori M., Burkert A., 2000, *ApJ*, 538, 559
- Navarro J. F., Eke V. R., Frenk C. S., 1996, *MNRAS*, 283, L72
- Navarro J. F., Frenk C. S., White S. D. M., 1997, *ApJ*, 490, 493
- Navarro J. F. et al., 2010, *MNRAS*, 402, 21
- Niederste-Ostholt M., Belokurov V., Evans N. W., Peñarrubia J., 2010, *ApJ*, 712, 516
- Ogiya G., Mori M., 2011, *ApJ*, 736, L2
- Ogiya G., Mori M., 2012, *ArXiv e-prints*
- Ogiya G., Mori M., Ishiyama T., Burkert A., 2014, *MNRAS*, 440, L71
- Oh S.-H., de Blok W. J. G., Brinks E., Walter F., Kennicutt, Jr. R. C., 2011, *AJ*, 141, 193
- Peñarrubia J., Pontzen A., Walker M. G., Koposov S. E., 2012, *ApJ*, 759, L42
- Pontzen A., Governato F., 2012, *MNRAS*, 421, 3464
- Prada F., Klypin A. A., Cuesta A. J., Betancort-Rijo J. E., Primack J., 2012, *MNRAS*, 423, 3018
- Press W. H., Schechter P., 1974, *ApJ*, 187, 425
- Richardson T., Fairbairn M., 2013, *ArXiv e-prints*
- Salpeter E. E., 1955, *ApJ*, 121, 161
- Salucci P., Burkert A., 2000, *ApJ*, 537, L9
- Salvadori S., Ferrara A., Schneider R., 2008, *MNRAS*, 386, 348
- Sheth R. K., Tormen G., 1999, *MNRAS*, 308, 119
- Spekkens K., Giovanelli R., Haynes M. P., 2005, *AJ*, 129, 2119
- Strigari L. E., Frenk C. S., White S. D. M., 2014, *ArXiv e-prints*
- Swaters R. A., Madore B. F., van den Bosch F. C., Balcells M., 2003, *ApJ*, 583, 732
- Takada M., 2010, in *American Institute of Physics Conference Series*, Vol. 1279, American Institute of Physics Conference Series, Kawai N., Nagataki S., eds., pp. 120–127
- Tegmark M. et al., 2004, *ApJ*, 606, 702
- Teyssier R., Pontzen A., Dubois Y., Read J. I., 2013, *MNRAS*, 429, 3068
- Tonini C., Lapi A., Salucci P., 2006, *ApJ*, 649, 591
- Tsuchiya M., Mori M., Nitta S.-y., 2013, *MNRAS*, 432, 2837
- van der Marel R. P., 2006, in *The Local Group as an Astrophysical Laboratory*, Livio M., Brown T. M., eds., pp. 47–71
- van Eymeren J., Trachternach C., Koribalski B. S., Dettmar R.-J., 2009, *A&A*, 505, 1
- Walker M. G., Mateo M., Olszewski E. W., Peñarrubia J., Wyn Evans N., Gilmore G., 2009, *ApJ*, 704, 1274
- Walker M. G., Peñarrubia J., 2011, *ApJ*, 742, 20
- Wang J., Frenk C. S., Navarro J. F., Gao L., Sawala T., 2012, *MNRAS*, 424, 2715
- Wolf J., Martinez G. D., Bullock J. S., Kaplinghat M., Geha M., Muñoz R. R., Simon J. D., Avedo F. F., 2010, *MNRAS*, 406, 1220